Malaysian Journal of Civil Engineering 29 Special Issue (2):265-283 (2017)

BOND DURABILITY OF STEEL PLATE TO CONCRETE PRISM USING STRUCTURAL ADHESIVES AFTER EXPOSURE TO 7-YEARS IN LABORATORY ENVIRONMENT

Nor Izzah Mokhtar[1]*, Shukur Abu Hassan[2], Abdul Rahman Mohd. Sam[1], Yusof Ahmad[1], Balqis Omar[1] & Ab Saman Abd Kader

[1]*Department of Structure and Materials, Faculty of Civil Engineering, Universiti Teknologi Malaysia, 81310 Skudai, Johor, Malaysia*
[2]*Centre for Composites (CfC), Institute for Vehicle and System Engineering (IVeSE), Universiti Teknologi Malaysia, 81310 Skudai, Johor Bharu, Malaysia*
[3]*Transportation Research Alliance, Universiti Teknologi Malaysia, 81310 Skudai, Johor, Malaysia*

*Corresponding Author: *mnorizzah@gmail.com*

Abstract: Structural integrity and durability has long been an area of study that is critical in order to ensure structures such as buildings, bridges etc. are safe enough to stand erected for many years. The technique of bonding steel plates to the surface of concrete using epoxy adhesives system has been used on a number of structures throughout the world to enhance load transferring capability. Deterioration in strength of concrete structures due to corrosion of steel can cause premature failure in existing structures or buildings. The objective of this study is to investigate the bond performance of steel to concrete using structural epoxy system. The sample at hand was prepared and left exposed for 7 years under normal ambient laboratory environments. This study focused on the outcome of bond performances of the bonded steel plate to concrete prism under pull out load. The sample (SPECS-7) that used in this study is approximately 7 years old with the steel plates surfaces was corroded and being compared with sample (SPECS-1) tested in 2008. The maximum load and maximum extension recorded at failure by sample SPECS-7 is 76.85kN and 3.04 mm at 181.8s which shows a decrease by 7 kN or 8% and 5.70 mm to 3.04 mm or 46% compared with sample SPECS-1 respectively. The extension comparison with SPEC-1 shows a reduction from 5.70 mm to 3.04 mm which is about 46 % less. There was significant amount of corrosion developed over the years which does not show to have affected the overall performance of the bonded system. Nevertheless, there was on average a small increase in bond strength with time although the controlled sample failed at a marginally lower load.

Keywords: *Epoxy bonding, steel plate, pull out Test, durability, tropical condition*

1.0 Introduction

Structural integrity and durability has long been an area of study that is critical in making sure structures such as buildings, bridges etc. are safe enough to stand erected for many years. Many studies have been conducted between different types of materials used to strengthened concrete structures. Strengthening of concrete structures using bonded steel plates are based on current experience and practice to provide external reinforcement. Deterioration in strength of concrete structures due to corrosion of steel can cause premature failure in existing structures or buildings and may force many structures need high cost of maintenance and rehabilitation throughout their service life (Broughton and Hutchinson, 2001).

The technique of bonding steel plates to the surface of concrete using epoxy resins adhesives has been used on a number of structures throughout the world to enhance load carrying capacity. Though the technique has been proved to be successful over the years, its application with concrete structures improves flexural, shear or compression capacity (Bakis *et al*., 2002; Mostofinejad and Shameli, 2011; Lorenzis *et al*., 2005; Setunge *et al*., 2002).

The long-term bond system performance and durability is still least reported in varies environmental condition to date (Sen, 2015; Davalos and Qiao, 2001). The main environmental causes influencing the bonding system during exposure is temperature and moisture (Smith, 2011). Weathering effect and mechanical loading also cause concrete structures to decay and deteriorate faster (Hassan *et al*., 2009). In a tropical climate like Malaysia, this is accelerated by the high humidity environment. Some researchers concerned on the behaviour, fatigue performance, debonding mechanism, creep effect and stiffness of bonding system in various environmental exposure such as natural climate, ocean environment (Abu Hassan *et al*., 2015; Zheng *et al*., 2015; Seracino *et al*., 2007; Dong *et al*., 2016; GangaRao and Vijay, 1998; Mostofinejad and Shameli, 2011).

Steel plate bonding helps in strengthening the structure externally without the need to demolish existing pillar or beams. The objective of this study is to investigate the bond performance of the bonded steel plate to concrete prism using structural epoxy system exposed to 7 years of laboratory environmental condition.

2.0 Methodology

The purpose of this study is to investigate and observe the outcome of adhesive bonded steel plate to concrete structure under push-pull test. The bond performance between the steel and concrete was compared to the results obtained in 2008 (Ling *et al*., 2008).The sample (SPECS-7) that used in this study is approximately 7 years old with the steel plates surfaces was corroded and being compared with sample (SPECS-1) tested in 2008.This section briefly describes on the methods used in sample preparations and testing procedures.

2.1 Concrete Prisms Specifications

The concrete mix proportions were designed according to DoE method. Concrete initial strength is set to be 40 N/mm^2.The dimension of concrete prism was 100 × 100 × 300 mm.

Table 1: DoE Mix Design Summary

Stage	*Item*	*Values*
1	1.1 Characteristic strength	40 N/mm^2 (28 days)
	1.2 Target mean strength	53.12 N/mm^2
	1.3 Water-cement ratio	0.46
2	2.1 Slump or Vebe time	100 mm
	2.2 Max aggregate size	10 mm
	2.3 Free-water content	250 kg/m^3
3	3.1 Cement content	543 kg/m^3
4	4.1 Assumed relative density of aggregate	2.65
	4.2 Concrete density (assumed)	2320 kg/m^3
	4.3 Aggregate content	1527 kg/m^3
5	5.1 Fine aggregate content	840 kg/m^3
	5.2 Coarse aggregate content	687 kg/m^3

Figure 1: Concrete prisms attached with G-clamp prepared in 2008

Figure 2: Concrete prisms prepared backed in 2008

2.2 Concrete Surface Preparation

The most common misconception in surface preparation is only need the clean surface. But actually, a clean surface is necessary condition for adhesion but not sufficient condition for bond durability. Most structural adhesive work as a result of the formation of chemical bonds (mainly covalent, but some ionic and static attractive bonds may also be present) between adherend surface atoms and compound constituting the adhesive. These chemical links are load transfer mechanism between the adherend.

So, these procedures must be followed. The grease and dust must be removed from all bonded surface by clean cloth. Then the bonding surface area is roughened using sand paper. The surface consider rough when the fiber filament emerge. The grease and dust shall be removed again by using acetone. Solvent degreasing is important because it removes contaminant materials which inhibit the formation of chemical bonds. However, solvent degreasing, whilst providing clean surface, does not promote the formation of acceptable surface conditions for longer term bond durability. This step clearly important because processing chemicals require contact with the substrate, and their effectiveness is diminished if the surface contaminated. In many cases, surface-modifying chemicals do not dissolve the contaminants, and an ineffective bond results if the solvent degreasing step is not perform adequately. Surface preparation should not be termed “cleaning” because it will lead to confusion between the different activities which combined to form the whole surface preparation process.

Initially, concrete prisms with good surface quality were chosen. The margins or borders were marked using masking tape. The bonding length of the steel plates is 200 mm. An extra 10 mm tolerance was provided around the bonding regions. Before the hacking process was carried out, one of the bonding edge was installed with a 10 mm steel plate, attached using G-clamp as shown in Figures 1 and 2. This was to protect the concrete edge from peeling off during the hacking process using air tool hammer and the depth of the hacked surface was around 2 mm. The preparation process of the concrete surface is shown in Figures 3 and 4.

Figure 3: Hacking with air tool hammer

Figure 4: Readily hacked concrete surface

2.3 *Plate to Concrete Prism Bonding*

The first step of the bonding works is the cleaning of the concrete surface as shown in Figure 5. The concrete prism was installed onto a specially made rig instrument for accurate bonding. A suitable amount of epoxy was applied onto the bonding surface and later the steel plate was pressed onto the epoxy. Excessive epoxy was removed and the edges were chamfered. An imposed load was applied as shown in Figures 5 and 6.

Figure 5: Surface cleansing to remove dust using air compressor

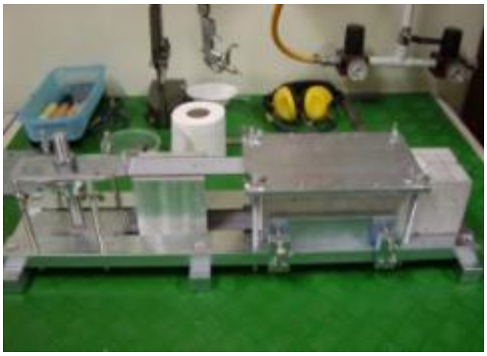

Figure 6: Jig used for proper bonding

2.4 *Specifications of Plates*

Steel plates were directly ordered from local supplier. The details specifications were shown in the Table 2.

Table 2: Typical properties of steel plates from supplier (Baldwins, 2011)

Material	*Thickness (mm)*	*Young's Modulus (GPa)*	*Tensile Strength (MPa)*	*Yield Strength (MPa)*
Mild Steel	5	200	Approximately 380 (can vary significantly)	230 (typical)

Figure 7 illustrates the dimension of the steel plate used for concrete bonding following the dimension used in 2008. The steel plates had to be sand blasted also for better bonding.

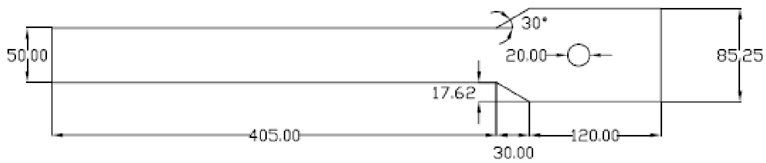

Figure 7: Steel Plate Dimensions

2.5 *Laboratory Environmental Conditions*

The creep and fatigue performance of adhesive connection will be influenced by the environmental conditions such as humidity, temperature and the level of applied stress. The in-service temperature of the adhesive joint should be below the 'safe working temperature' which is 10° to 20° below the glass transition temperature. High ambient temperatures will cause the adhesive to creep. As a rule the sustained stress in an adhesive bonded joint should be kept below 25% of the short term strength of the joint for the normal design life of the structure. Samples SPECS-1 and SPECS-7 were prepared at the same time but sample SPECS-7 was subjected to laboratory environment exposure for 7 years. The temperature and relative humidity fluctuated between 25–32°C and 75–90%, respectively experienced by the sample.

2.6 *Material Preparation*

The sample (SPECS-7) that was used in this study is approximately 7 years old with the steel plates outer surface was corroded and being compared with sample (SPECS-1) tested in 2008. However, before undergoing tests, the steel plate has to be de-rusted and cleaned from any form of impurities for strain gauges installation. Figure 8shows the 7-year sample with corroded steel plates. Figures 9 to 11(b) show the sample preparations prior load test.

Figures8: SPECS-7 with corroded steel plate

Figure 9: SPECS-7 before the application of rust remover

Figure 10: SPECS-7 after the application of rust remover

(a)

(b)

Figure 11: Degreasing process by the rust remover takes time within 2 hours

Prior to the installation of strain gauges, the roughening process of steel plate's surface using sand paper grade 400 was performed. In order to remove the dirt, acetone was rubbed on steel plates. After the installation process, the gauges were left for 24 hours for curing before testing. Later, extension wires were joined to the gauge terminal by shouldering method.

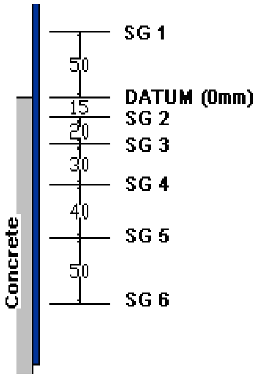

Figure 12: Strain gauges locations along bond length

Figure 13: Sample SPECS-7 after installation of strain gauges

2.7 Test Set-Up

After all the necessary preparation work, SPECS-7 was installed in the way as shown in Figures 14 to 16. A tensile load was applied vertically until failure. All wires linking to the strain gauges were connected to a data logger to render the readings.

Figure 14: Instron 5982 Universal Testing Machine

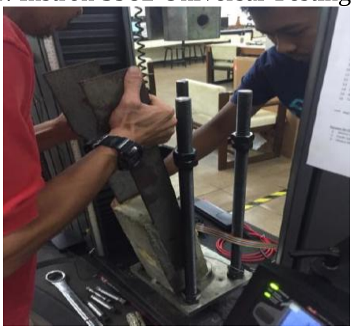

Figure 15: Installation of pull-out test rig

Figure 16: Sample ready for loading

3.0 Results and Discussion

The discussion focuses on the outcome of tensile test on the experimentation sample (SPECS-7) which has been exposed for duration of 7 years in a controlled laboratory environment. Comparisons are made between the results obtained for samples SPECS-7 and SPECS-1.

Sample SPECS-7 was tested under tensile load. By referring to Figure 17, the maximum load recorded at failure is 76.85kN. Dividing the applied load by two, the load for one side of the plate is 38.42kN. The maximum extension for the sample is 3.04mm at 181.8s comparing this data with that of sample SPECS-1 test, load for the sample SPECS-7 in this study shows a decrease by 7kN or 8%. The time taken and extension also show to be decreased in this sample. The extension comparison with sample SPECS-1 shows a reduced difference from 5.70mm to 3.04mm which is 46% less. This may be due to early failure at the bond.

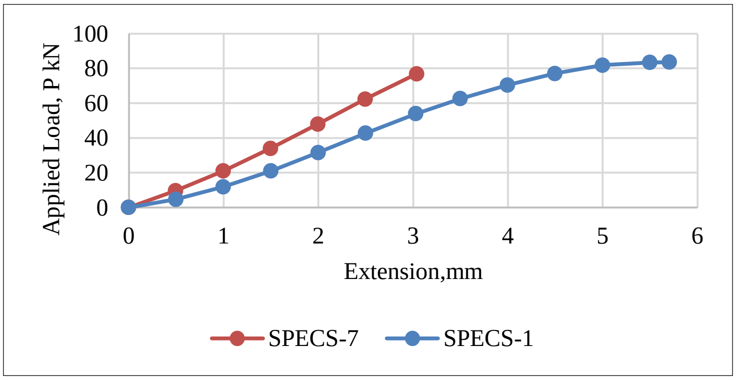

Figure 17: Load versus extension comparison between samples SPECS-7 and SPECS-1

In Figure 17, it can be seen how the bond between the adherents and adhesive behave. Sample SPECS-7 shows to have a much more abrupt failure halfway through the total amount of time taken for sample SPECS-1 to fail. The curved graph for SPECS-1 also can be seen to be more ductile as the load increases, the extension follows uniformly until failure. SPECS-7 shows brittle behavior indicated by the linear line of the curve.

3.1 Strain Analysis

The strain readings were taken at the interval of every 5kN. Six strain gauges were installed to sample SPECS-7 prior to the testing. The graph of total applied load versus local strain is shown in Figure 18. It was found that the strain distribution along the bond length was generally linear, i.e. proportional to the applied load and uniform. Strain gauges 2, 3 and 4 shows that the Local bond stresses are higher compared to strain gauges 1, 5 and 6. We can say that this is due to the close proximity to the datum. Furthermore, the distance between each of the strain gauges along the bonding surface also indicates bond stress distributions. Strain gauge 2(SG2), being the closest to the datum, is distinctive from other gauges in terms of strain values recorded.

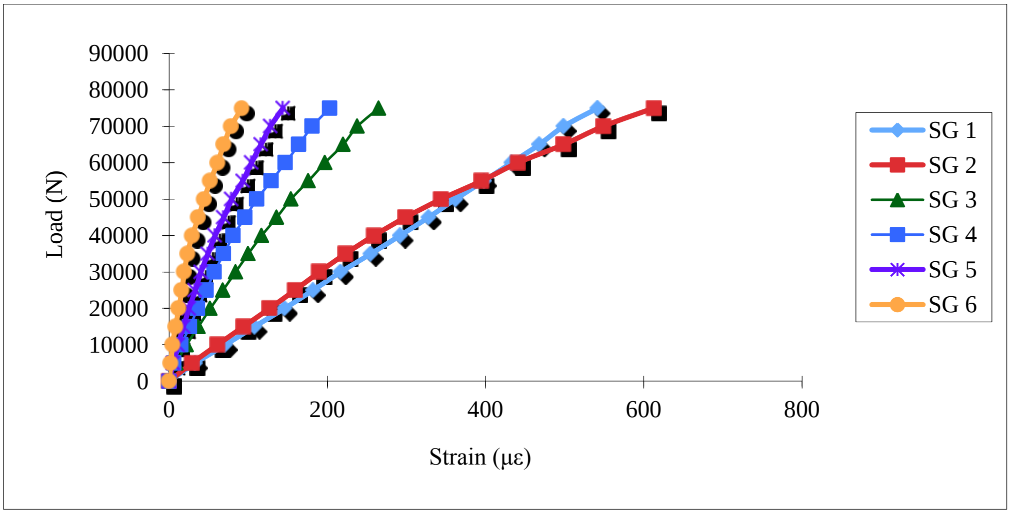

Figure 18: Load versus Strain for SPECS-7

3.2 Local Bond Stress

The local bond stress distributions along the bonded length can be determined by assuming a linear variation of the longitudinal force along the Steel Plate between two consecutive strain gauge locations. Local steel plate force at any location along the bond length can be determined by equation [1].While, the local average bond stress between two consecutive gauges position can be determined by equation [2] by referring to two strain readings $\hat{A}_{i/steel}$and $\hat{A}_{j/steel}$at position $i$and j, the plate thickness t_p, its elastic Young modulus E_{steel}, and the distance $f_{Li\text{-}j}$ between two consecutive strain gauges positions. Steel Plate local force at i location,

$$F_{steel,i} = \delta U\,(W \times t)$$

$$F_{steel,i} = E_{steel}\,A_i\,(W \times t) \qquad [1]$$

$$U_{i\text{-}j} = (F_{steel,i} - F_{steel,j})/(\delta x \times w) \qquad [2]$$

where,

w	=	Steel plate width (mm)
t	=	Steel plate thickness (mm)
$f_{Li\text{-}j}$	=	δx = the distance between two consecutive strain gauges $(F_{steel,i} - F_{steel,j}) = f_{Fi\text{-}j}$ = the variation of the local longitudinal force.
E_{steel}	=	steel plate Young's Modulus (GPa).
$\hat{A}_{i/steel}$	=	steel plate Local Strain at Point, i (µÂ).

Table 3 shows the material parameters values used to apply the mentioned equations above to calculate local bond stress and local load values.

Table 3: Material properties

Parameter	*Value*
Epoxy shear modulus, G_a(GPa)	2.7
Steel Plate Young's modulus, E_{steel}(GPa)	200
Concrete Young's modulus, $E_{concrete}$(GPa)	30
Thickness of epoxy, t_a(mm)	1.5
Thickness of Steel Plate t_{steel}(mm)	5
Thickness of concrete, $t_{concrete}$(mm)	100
Bond length, L (mm)	200

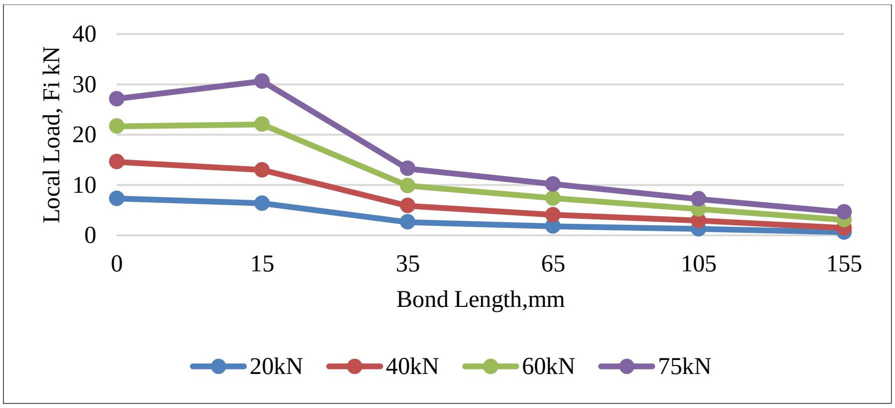

Figure 19: Local Load versus Bond Length for SPECS-7

From Figure 19, it is observed that the local loads are higher in the beginning of the bond length. As the bond length increases pass the 35mm mark, there is linear decrease in the local load distributions. This may well indicate that at the earlier lengths of bond, the force transfer from the steel plate to the adhesive is very much high and the bulk of the stress are concentrated at this region. The distribution of local forces in the 0 to 35 mm bond region clearly shows an exponential trend as compared to results from sample SPECS-1.

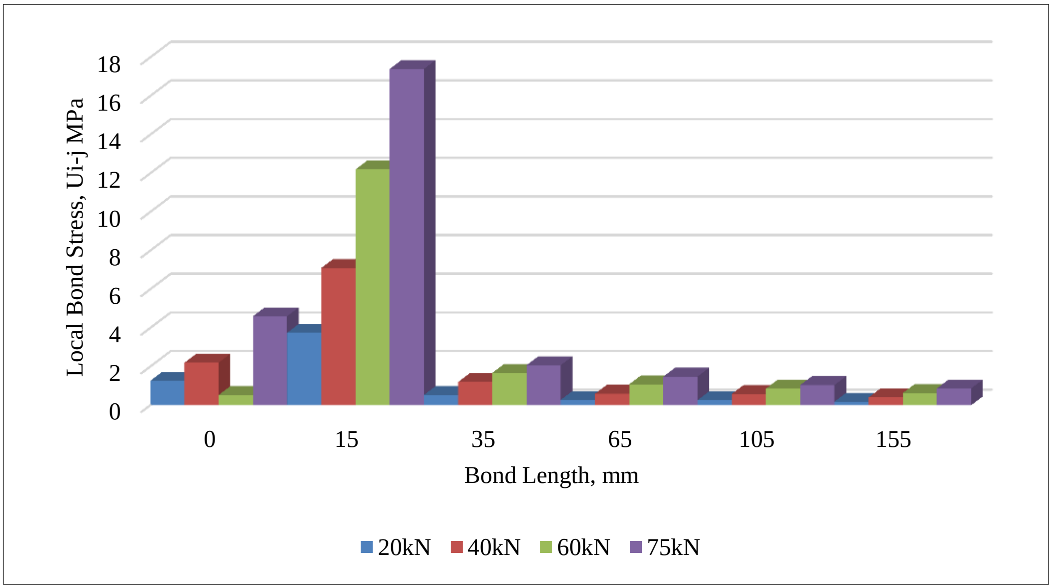

Figure 20: Local Bond Stress versus Bond Length at various load levels for SPECS-7

As shown in Figure 20 above, comparisons of the local bond stresses are made between the different load levels. As previous test for SPECS-1 prove, the local bond stresses are significantly high at the end of the bond lengths. The stresses recorded at 35mm to 105mm mark, tells us that the force distribution is much more uniform across the centre bond length of the plates.

3.3 Comparison with Sample SPECS-1

From the data obtained by test conducted to sample SPECS-1, we can compare the information and investigate the reason behind the different end results. Figure 21 illustrates a comparison between two samples at 20kN load level. Clearly from the graph, it is shown that SPECS-1 specimen underwent relatively higher stress values and the curved graph indicates that the distribution of local longitudinal forces and shear stress along the bond are exponential. For SPECS-7, The trend is almost the same except for lower bond stress values recorded. SPECS-1 also shows much more uniformly distributed stresses along the bond length.

Figure 22 indicates increase values in shear stress as expected when the load increases. At 40kN the trend remains the same for SPECS-7 with the values decreasing as the gauges are further apart from the datum. It can be said the same for the 60kN and 75kN loads in Figures 23 and 24 respectively. The lower values recorded by SPECS-7 could be because of the reduced bond strength between Steel-Epoxy rather than the epoxy-concrete bond. However, for SPECS-1 we can see from the graphs that micro cracking may occurred at bond lengths 15mm to 35mm where the graph tends to distort from the uniform shape. In Figures 24 and 25 respectively, the micro cracking occurring within SPECS-1 shows some linearity from 15mm to 35 mm length. This indicates the propagation of the cracking from corresponding lengths after total shearing of the bond interfaces at 0mm to 15mm.

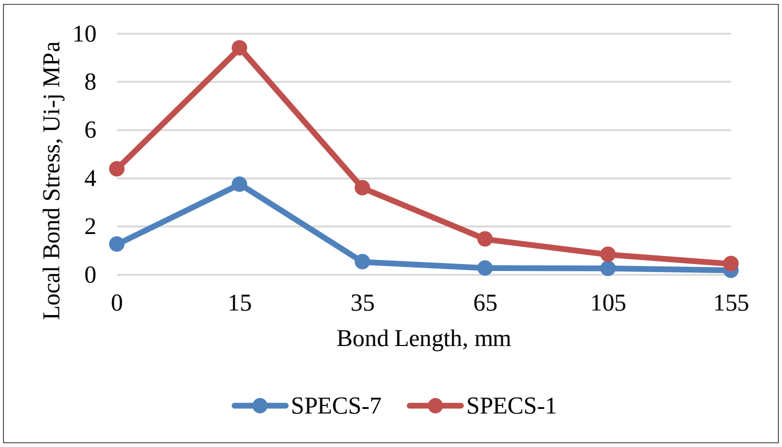

Figure 21: Comparison at 20kN Load level for SPECS-7 and SPECS-1

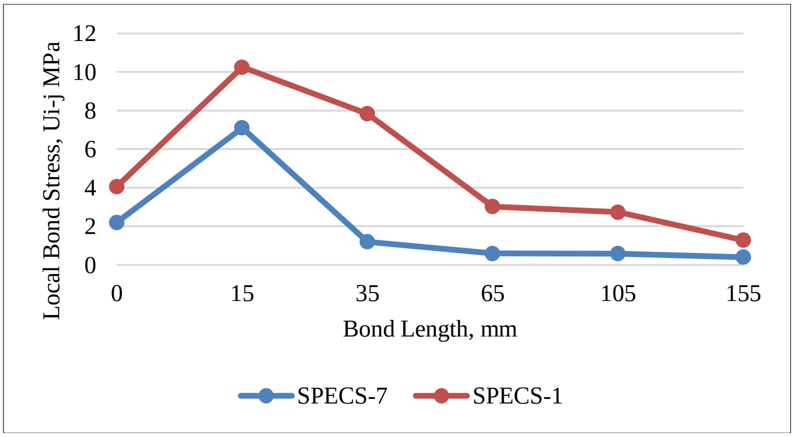

Figure 22: Comparison at 40kN Load level for SPECS-7 and SPECS-1

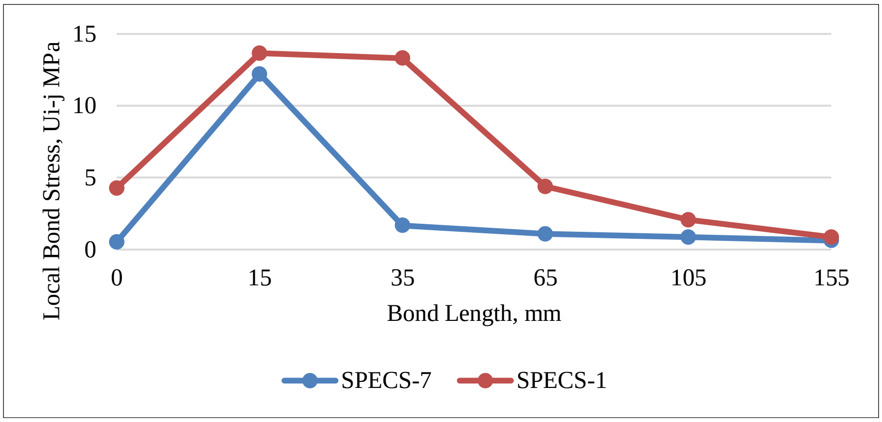

Figure 23: Comparison at 60kN Load level for SPECS-7 and SPECS-1

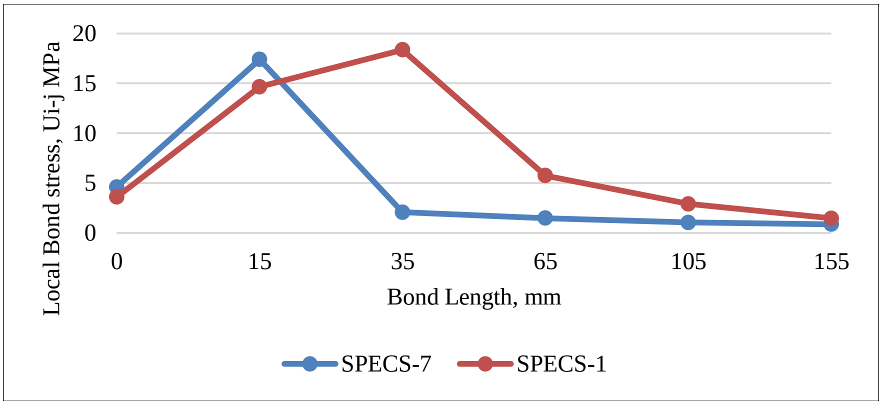

Figure 24: Comparison at 75kN Load level for SPECS-7 and SPECS-1

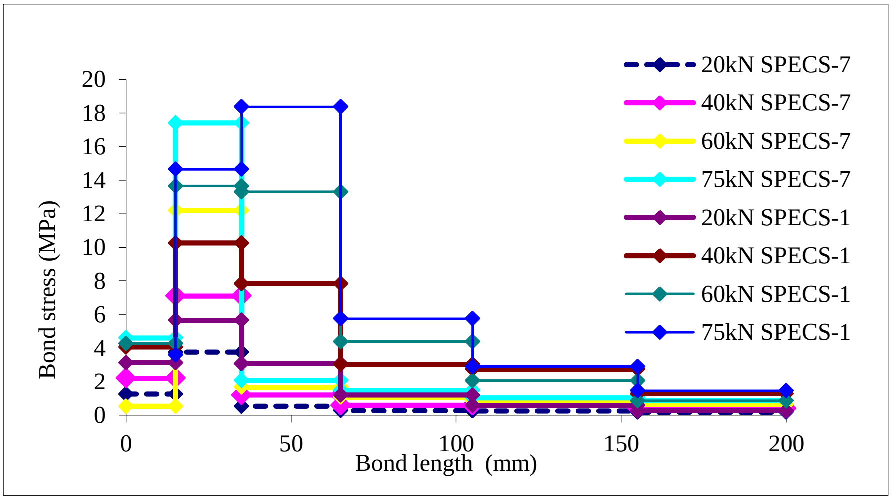

Figure 25: Comparison of local bond stress versus bond length between SPECS-7 and SPECS-1

Figure 25 above presents a comparison on local bond stress at various bond length between SPECS-7 and SPECS-1. The stress distributions along the bond length show that for SPECS-7, the local bond stresses are much lower and linear towards the end of the bond length. Sample SPECS-7 also recorded lower local bond stresses at the same applied loads as compared to SPECS-1.

At all load levels indicated, SPECS-7 recorded lower local bond stress levels. Although SPECS-1 bond failure occurred at double the amount of time recorded for SPECS-7, this shows that the bond strength at a much matured ageing period is far stronger that a 1 month old specimen. We can say from the data provided, that SPECS-7 bond is brittle and hard and SPECS-1 has a much more ductile behaviour.

At failure, only one side of the bonded prism separated due to localized shear stresses between the steel plate and the epoxy. We can assume that the data obtained is consistent on both steel plates. Figures26(a) and (b) shows the separation that happened right at failure. The reason may be due to small difference in comparison. Although the debonding occurred on the steel plate without any strain gauge, The difference in recorded data is negligible as stated in previous studies of similar materials(Mohamed, 2007). From here we can assume that the strain values recorded are the same. Inspecting the condition of the steel plate and concrete prism after removing the specimen from the test machine, Figure 27 shows the bulb formation of concrete on the steel plate specimen. The remaining bonded surface area remains clean of oxides, residual epoxy and concrete.

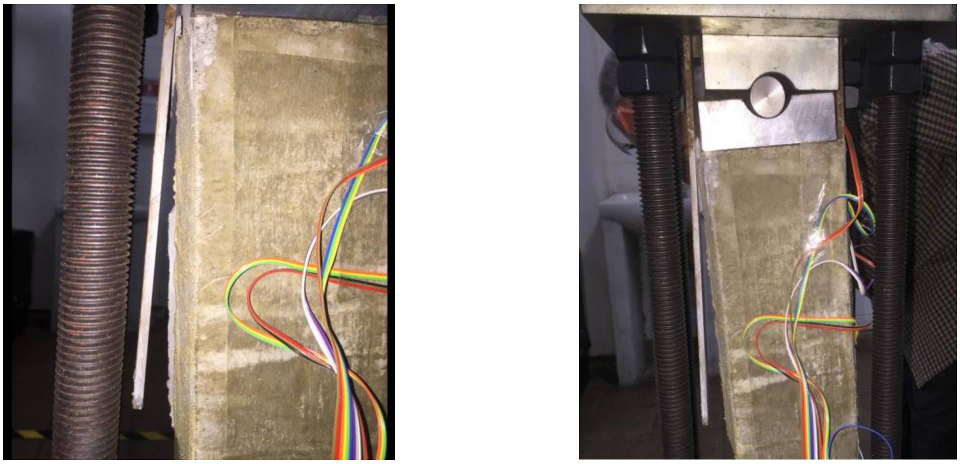

(a) (b)

Figure 26: Debonding on one side of the concrete prism of SPECS-7

Figure 27: Formation of concrete bulb on steel plate after failure

Figure 28: Concrete from SPECS-7 after failure

The failure zones suggest that failure was a combination of adhesion at the steel – epoxy interface and cohesion due to epoxy failure. The 7 year aging of the bond between both epoxy and concrete may have shown encouraging signs, but the steel to epoxy bond is suspect in bond suitability of both materials. Comparing the data obtained from the strain gauges, we can relate the high strains recorded at the gauges closest to the datum. The physical observation of the specimen verifies this as the concrete fracture across bond lengths 0mm to 35mm.

4.0 Conclusions

The double lap joint system of Steel Plate-epoxy-Concrete tested for durability represented by sample SPECS-7 provided some very interesting results for comparison with previous test results represented by sample SPECS-1. There was significant amount of corrosion developed over the years which does not show to have affected the overall performance of the bonded materials. Nevertheless, there was on average a small increase in strength with time although the controlled specimen failed at a marginally lower load.

The epoxy bonding on concrete proved to be strong even after 7 years in controlled laboratory environment. A thicker and more durable steel plate need to be used in future study. The ultimate load at failure of sample SPECS-7 is observed to be lower by 12% compared to sample SPECS-1. Same goes to the time taken to achieve ultimate load and extension at failure show decrease pattern compared to SPECS-1.

The bond force transfer from steel plate to concrete was linear and occurred at uniform rate with no yielding of steel plates as an evident. This may well indicate that at the earlier lengths of bond which is from 0 to 35 mm bond region, the force transfer from the steel plate to the adhesive is very much high and the bulk of the stress are concentrated at this region. As previous studies prove, the local bond stresses are significantly high at the end of the bond lengths which is at 35 mm to 105 mm bond length. These results may lead to the conclusion that the force distribution is much more uniform across the centre bond length of the plates. Further study need to be done on the effect of moisture and corrosion ingression to the bond durability between steel or other strengthening materials to concrete surface.

5.0 Acknowledgements

The authors would like to thank Universiti Teknologi Malaysia for funding this research and UTM Research Management Centre (RMC) for managing the research activities under Vote 10H22.

References

Abu Hassan, S., Gholami, M., Ismail, Y. S., & Mohd Sam, A. R. (2015). Characteristics of Concrete / CFRP Bonding System Under Natural Tropical Climate. *Construction and Building Materials*, *77*(July), 297–306.

Bakis, C. E., Bank, L. C., Brown, V. L., Cosenza, E., Davalos, J. F., Lesko, J. J., … Triantafillou, T. C. (2002). Fiber-Reinforced Polymer Composites for Construction—State-of-the-Art Review. *Journal of Composites for Construction*, *6*(2), 73–87.

Baldwins, R. (2011). *Mild Steel Product Guide*.

Broughton, J. G. U., & Hutchinson, A. R. (2001). Effect of timber moisture content on bonded-in rods, (February 2000).

Davalos, J. F., & Qiao, P. (2001). Interface Durability of Construction Materials Externally Reinforced with FRP Composites.

Dong, Z., Wu, G., & Xu, Y. (2016). Experimental study on the bond durability between steel-FRP composite bars (SFCBs) and sea sand concrete in ocean environment. *Construction and Building Materials*, *115*, 277–284.

GangaRao, H. V. S., & Vijay, P. V. (1998). Bending Behavior of Concrete Beams. *Journal of Structural Engineering*, *6*(January), 3–10.

Hassan, S. A., Ismail, Y. S., & Sam, A. R. M. (2009). Load sustained rig for bond durability study. *Jurnal Mekanikal*, *28*(June), 16–27.

Ling, P. C. C., Sam, A. R. M., & Hassan, S. A. (2008). *Bonding Behavior between CFRP and Steel Plates to Concrete Prisms*.

Lorenzis, L. De, Scialpi, V., & Tegola, A. La. (2005). Analytical and experimental study on bonded-in CFRP bars in glulam timber. *Composites Part B: Engineering*, *36*(4), 279–289.

Mohamed, K. b. (2007). *The development of a Mathematical Model for predicting bonding behaviour of CFRP Plate-Epoxy-Concrete Bonded System*. Universiti Teknologi Malaysia.

Mostofinejad, D., & Shameli, M. (2011). Performance of EBROG Method under Multilayer FRP Sheets for Flexural Strengthening of Concrete Beams. *Procedia Engineering*, *14*, 3176–3182.

Sen, R. (2015). Developments in the durability of FRP-concrete bond. *Construction and Building Materials*, *78*, 112–125.

Seracino, R., Jones, N. M., Ali, M. S. M., Page, M. W., & Oehlers, D. J. (2007). Bond Strength of Near-Surface Mounted FRP Strip-to-Concrete Joints. *Journal of Composites for Construction*, *11*(August), 401–409.

Setunge, S., Nezamian, A., & Lokuge, W. (2002). *Review of strengthening techniques using externally bonded fiber reinforced polymer composites*.

Smith, S. T. (2011). Strengthening of Concrete, Metallic and Timber Construction Materials with FRP Composites. *The 5th International Conference on FRP Composites in Civil Engineering (CICE 2010)*, 13–19.

Zheng, X. H., Huang, P. Y., Chen, G. M., & Tan, X. M. (2015). Fatigue Behavior of FRP–Concrete Bond Under Hygrothermal Environment. *Construction and Building Materials*, *95*, 898–909.